2012

Scaling law for direct current field emission-driven microscale gas breakdown

A Venkattraman

Alina A. Alexeenko
Purdue University - Main Campus, alexeenk@purdue.edu

Recommended Citation
Venkattraman, A and Alexeenko, Alina A., "Scaling law for direct current field emission-driven microscale gas breakdown" (2012). *School of Aeronautics and Astronautics Faculty Publications.* Paper 11.
http://dx.doi.org/10.1063/1.4773399

Scaling law for direct current field emission-driven microscale gas breakdown

A. Venkattraman and A. A. Alexeenko

Citation: Physics of Plasmas **19**, 123515 (2012); doi: 10.1063/1.4773399
View online: http://dx.doi.org/10.1063/1.4773399
View Table of Contents: http://scitation.aip.org/content/aip/journal/pop/19/12?ver=pdfcov
Published by the AIP Publishing

Scaling law for direct current field emission-driven microscale gas breakdown

A. Venkattraman and A. A. Alexeenko[a)]
School of Aeronautics & Astronautics, Purdue University, West Lafayette, Indiana 47907, USA

(Received 13 August 2012; accepted 11 December 2012; published online 28 December 2012)

The effects of field emission on direct current breakdown in microscale gaps filled with an ambient neutral gas are studied numerically and analytically. Fundamental numerical experiments using the particle-in-cell/Monte Carlo collisions method are used to systematically quantify microscale ionization and space-charge enhancement of field emission. The numerical experiments are then used to validate a scaling law for the modified Paschen curve that bridges field emission-driven breakdown with the macroscale Paschen law. Analytical expressions are derived for the increase in cathode electric field, total steady state current density, and the ion-enhancement coefficient including a new breakdown criterion. It also includes the effect of all key parameters such as pressure, operating gas, and field-enhancement factor providing a better predictive capability than existing microscale breakdown models. The field-enhancement factor is shown to be the most sensitive parameter with its increase leading to a significant drop in the threshold breakdown electric field and also to a gradual merging with the Paschen law. The proposed scaling law is also shown to agree well with two independent sets of experimental data for microscale breakdown in air. The ability to accurately describe not just the breakdown voltage but the entire pre-breakdown process for given operating conditions makes the proposed model a suitable candidate for the design and analysis of electrostatic microscale devices. © *2012 American Institute of Physics*. [http://dx.doi.org/10.1063/1.4773399]

I. INTRODUCTION

Field emission[1] refers to the emission of electrons from the cathode due to the application of intense electric fields typically greater than 100 V/μm. The emission of electrons lead to different effects depending on whether the emission is in vacuum or in the presence of an ambient neutral gas. The various aspects of electron emission in vacuum have been analyzed in detail in the past.[2–4] The negative space charge that accumulates due to the emitted electrons suppresses the electric field and hence the current density of electrons eventually leading to a space charge limited current density.[3] However, when field emission occurs in the presence of an ambient neutral gas, a fraction of the emitted electrons gain sufficient energy in the electric field leading to the ionization of neutral atoms, thereby generating ions and resulting in the formation of a Townsend dark discharge. Depending on operating conditions, this could eventually lead to gas breakdown through an electron avalanche.[5]

The scaling law for traditional macroscale gas breakdown is given by the Paschen curve.[6] The Paschen curve predicts a minimum breakdown voltage of about 300 V for air (for a typical secondary electron emission coefficient of 0.01) at atmospheric pressure occurring for a gap size of about 10 μm. For micron-sized gaps that are, for example, frequently encountered in microscale devices in the electronics industry, the Paschen law predicts a breakdown voltage of a few kV. As a result, gas breakdown was not considered to be a possible breakdown mechanism in microgaps that typically have a few 100 V applied across them. However, experiments in the past[7–10]—summarized in detail by Go and Pohlman[11] and not repeated here—have observed glows, sparks, and other charging phenomena in microgaps of various gases at few tens of volts, which is much lower than the minimum predicted by the Paschen curve.

This deviation has been attributed to the field emission of electrons, thereby leading to the formation of a self-sustained field emission-driven microdischarge. In order to describe gas breakdown for all gap sizes, a modification to the Paschen curve has been proposed by including the effects of field emission in microgaps and is commonly referred to as the *modified Paschen curve*.[12] The modified Paschen curve bridges the purely field emission-induced breakdown at very small gaps to the traditional Paschen curve-predicted breakdown. Obtaining analytical models that describe this transition accurately has been an active area of research in the recent past due to, for example, their importance in predicting the reliability of electrostatically actuated microelectromechanical systems (MEMS) including sensors and actuators.

Radmilovic-Radjenovic *et al.* have published a series of papers[13–15] considering numerical simulations to predict the breakdown voltage in small gaps including the effects of field emission. Data from experiments[16] performed using structures with a gap size of about 3 μm were explained[17] using the particle-in-cell/Monte Carlo collisions (PIC/MCC) simulations to extract parameters that describe the breakdown process as opposed to just the breakdown voltage. However, with the simulations performed for a fixed set of parameters, they lack the predictive capability that is likely

a)Electronic mail: alexeenk@purdue.edu.

to be important to the analysis of electrostatic microscale devices. While the lack of predictive capability has been addressed partially by the mathematical models presented by Go and Pohlman[11] and Tirumala and Go,[18] they still have their limitations. With approaches completely based on theory,[18] parameters such as ionization coefficient extrapolated from macroscale behavior coupled with other assumptions related to location of formation of ion make these approximate models. On the other hand, the model described by Go and Pohlman[11] involves an arbitrary fitting parameter, K, obtained from experiments which decreases the predictive capability. The disadvantage due to the arbitrary fitting parameter has been partially addressed recently by Rumbach and Go[31] where they formulate a model for K by considering the non-dimensional Poisson's equation and deriving an approximate ion number density that leads to avalanche breakdown. However, while their fluid model solved numerically describes the pre-breakdown current densities accurately, their approximate analysis to predict pre-breakdown characteristics starts deviating from the fluid model at about 20 V below the breakdown voltage, which is crucial considering that the current densities at lower voltages are anyway negligible.

Therefore, there is still a need for a compact model that can accurately predict the breakdown voltage as well as pre-breakdown current-voltage characteristics of microgaps without the use of uncertain fitting parameters, theories extended based on behavior at macroscales, or detailed numerical simulations. The main goal of this work is to address this issue by formulating, and validating using fundamental PIC/MCC numerical experiments, a scaling law that can not only predict the breakdown voltage but also describe the entire breakdown process in microgaps using parameters relevant to microscale. The advantages of such a model would be its potential application in the design and analysis of electrostatic microscale devices without having to repeat a large number of PIC/MCC simulations to determine the breakdown voltage for a given microscale device. The remainder of the paper is organized as follows; Sec. II provides the necessary theory and background; Sec. III presents the model formulation, results and discussion with Sec. IV reserved for the conclusions.

II. THEORY AND BACKGROUND

The generation of ions in microgaps has been a widely studied problem for a variety of applications including gas sensors, electronic cooling pump,[19] and electrostatic micromotors.[10] Traditionally, as described in Sec. I, the breakdown of gases by production of charged particles is described by the Paschen curve,[6] which relates the breakdown voltage to the pressure and gap size between the anode and cathode. The breakdown voltage is derived using the Townsend avalanche criterion

$$\gamma_{se}(e^{\alpha d} - 1) = 1, \tag{1}$$

where γ_{se} is the secondary electron emission coefficient, which represents the probability of electron emission when an ion strikes the cathode. In Eq. (1), α is the ionization coefficient defined as the number of ions generated per electron per unit length. Traditionally α is described by the semi-empirical relation[6]

$$\alpha = A_p p \exp\left(-\frac{B_p p}{E}\right), \tag{2}$$

where p is the pressure, E is the electric field, A_p and B_p are gas-dependent parameters that are usually obtained using experimental data for α performed on macroscale gaps around 1 mm. Using Eq. (2) in Eq. (1) gives an expression for macroscale breakdown voltage (V_b), which is referred to as the Paschen law and is given by

$$V_b = \frac{B_p p d}{\log(A_p p d) - \log(\log(1 + 1/\gamma_{se}))}. \tag{3}$$

It has now been well established that field emission plays a major role in gas breakdown at microscales. The process of field emission is quantitatively described by the Fowler-Nordheim (F-N) theory,[20] which relates the current density of field emitted electrons to the electric field using the equation given by

$$j_{FN} = \frac{A_{FN}\beta^2 E^2}{\phi t^2(y)} \exp\left(-\frac{B_{FN}\phi^{3/2} v(y)}{\beta E}\right), \tag{4}$$

where ϕ is the work function of the cathode material, β is the field enhancement factor, and A_{FN} and B_{FN} are constants. $v(y)$ and $t^2(y)$ were not part of the original F-N equation and were corrections included later.[21] The correction terms are given by

$$v(y) \approx 0.95 - y^2,$$

$$t^2(y) \approx 1.1,$$

where $y \approx 3.79 \times 10^{-4}\sqrt{(\beta E)}/\phi$ is a function of the electric field, work function of the cathode, and the field enhancement factor. The field enhancement factor β is a strong function of the surface properties including roughness. The dependence on roughness makes it hard to predict the value of β whose values have been found to vary between 1.5 and 115 in various experiments in the past.[22] Previous work[19] dealing with numerical simulations of ion generation in micron gaps of air used a value of around 50.

The mathematical model for the modified Paschen curve is an attempt to derive an expression for breakdown voltage including the effects of field emission. Therefore, the Townsend avalanche criterion in Eq. (5) used to obtain the Paschen curve is modified as[11]

$$(\gamma_{se} + \gamma')(e^{\alpha d} - 1) = 1, \tag{5}$$

where γ' is the ion-enhancement coefficient used to capture the influence of field emission and its enhancement due to positive space charge. This work makes an attempt to formulate a unified scaling law based on a theoretical analysis that considers a steady-state one-dimensional microdischarge and

derives an expression for the pre-breakdown current density as well as a new breakdown criterion that describes gas breakdown in both microscale and macroscale gaps. The numerical experiments used to validate the proposed scaling law are performed using the PIC/MCC method, which is explained in detail by various researchers in the past.[23–25] In this work, the open source one-dimensional PIC/MCC code XPDP1[26] developed at the University of California, Berkeley, has been used after including the effects of field emission. The number of electrons emitted from the cathode was determined using the F-N equation using the local value of the electric field and a fixed value of β.

III. RESULTS AND DISCUSSION

This section presents details of the formulation of models used in the current work. Initially, the microscale ionization coefficient, α, is considered followed by an analysis of the effects of positive space charge enhancement of field emission.

A. Microscale ionization coefficient

The method used to obtain α using PIC/MCC numerical experiments is described below. A constant current source is introduced at the cathode and the total current density in the gap and the ion and electron current densities at the cathode at steady state are obtained. The steady state total current density in the gap is related to the current density of the cathode source by the relation[6]

$$j = j_0 \exp(\alpha d), \tag{6}$$

where j is the steady state current density in the gap and j_0 is the current density of the cathode source. The value of α can be obtained from the known values of j, j_0, and d. However, the above expression does not account for the small decrease in electron current density at the cathode due to backscattering particularly for low applied voltages. Therefore, a more accurate method to estimate α would be to use the ratio of ion to electron current density at the cathode as

$$\frac{j_i}{j_e} = \exp(\alpha d) - 1. \tag{7}$$

Here, the value of j_e is slightly less than j_0. It should be mentioned that in these simulations, the value of γ_{se} was set as 0. For a non-zero value of γ_{se}, the steady state current density is related to the current density of the cathode source as[6]

$$j = \frac{j_0 \exp(\alpha d)}{1 - \gamma_{se}(\exp(\alpha d) - 1)}. \tag{8}$$

Before determining the values of α for microscale gaps, it is important to verify that the behavior of α is indeed different in microscale gaps when compared to macroscale gaps. If microscale ionization coefficient follows the empirical law in Eq. (2), it is clear that, for a given pressure, α is a function only of the electric field and not of voltage and gap independently. Therefore, the value of α should be the same for 0.5, 1, and 2 μm as long as the applied electric field and pressure were the same. This was tested using PIC/MCC simulations performed for gap sizes of 0.5, 1, and 2 μm filled with argon at applied voltages of 25, 50, and 100 V, respectively, all of which correspond to an electric field of 50 V/μm. The simulations were performed for a cathode source current density of 616.49 A/m^2, which corresponds to the F-N current density at an electric field of 50 V/μm. It should be mentioned that, for these simulations, any small current density value could have been used.

Figure 1 shows the variation of number density of ions and electrons across the gap for gap sizes of 0.5 and 2 μm. Since the results are based on particle methods, instantaneous values of macroscopic quantities are noisy, and all results presented were based on about 500 000 sampling timesteps after the system reached steady state. The ratio of real to computational particles was chosen for each case such that the total number of computational ion particles (the species with higher number density) was around 0.1×10^6 at steady state. The timestep was chosen as 10^{-15} s, which ensures that a computational particle does not cross several cells in one timestep with the cell size being chosen as

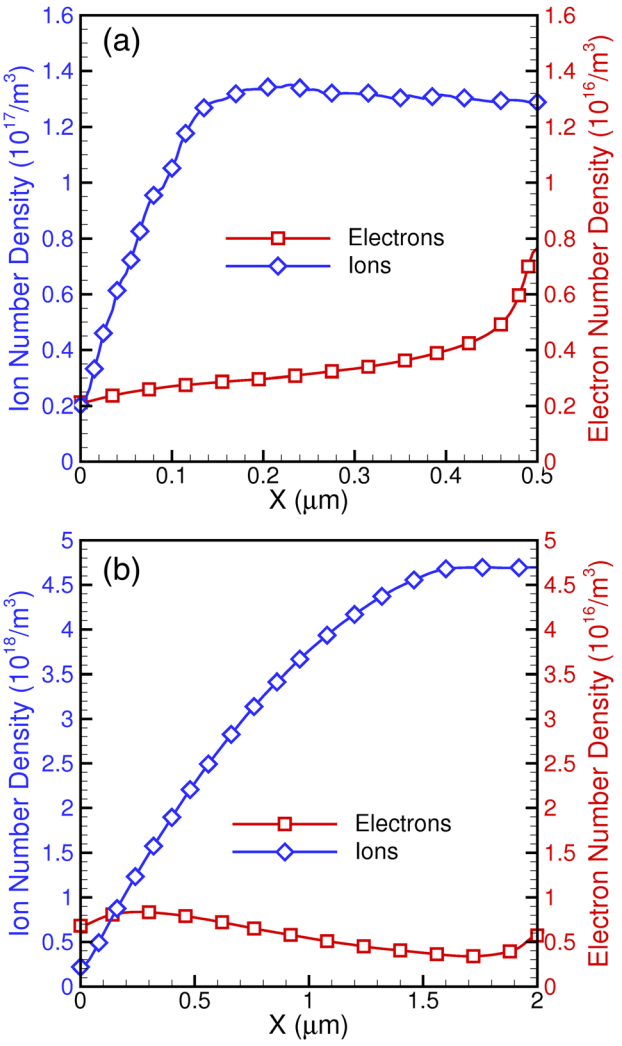

FIG. 1. Comparison of ion and electron number density variation across the gap for 0.5 and 2 μm argon microdischarge at an electric field of 50 V/μm. $j_0 = 616.49$ A/m^2 and $\gamma_{se} = 0.0$; (a) is 0.5 and (b) is 2 micron.

0.01 μm. The number densities shown in Figure 1 show that the net charge in the gap is positive with the ion number density higher than the electron number density by at least one order of magnitude depending on the gap size. The higher ion number density is due to a lower free diffusion for ions and the absence of a quasi-neutral region ensures that there is no ambipolar diffusion.[27]

Figure 2 shows the variation of electron, ion, and total current density across the gap for 0.5 and 2 μm gaps. It can be observed that electrons carry almost all the current at the anode whereas the current density is shared between electrons and ions at the cathode. The ratio of electron to ion current density at the cathode is about 15 for the 0.5 μm gap and decreases to 0.43 for the 2 μm gap. The ratio of electron to ion current density at the cathode is $1/(\exp(\alpha d) - 1)$ and for small gaps, $\exp(\alpha d)$ is just above 1 resulting in a large electron to ion current density. It should be mentioned that in the case of very small gaps where no ionization occurs, there are no ions generated and electrons carry all the current in the entire gap. A similar scenario holds true even for larger gaps when the conditions in the gap are close to vacuum implying that there are no neutrals to be ionized.

The value of α, as described before, is obtained using the ratio of ion to electron current density at the cathode. For the 0.5 μm gap, the value of α at an electric field of 50 V/μm was obtained as 1290.18 1/cm. For the 2 μm gap at 100 V, α was obtained as 6005.50 1/cm. It was also ensured that the electric field variation across the gap is not significant for all the simulations. If the electric field variation is significant, the value of α obtained from the PIC/MCC simulations will not correspond to an electric field of 50 V/μm but will correspond to an average value across the range of electric fields encountered in the gap. Figure 3 shows the potential and electric field variation across the gap for both 0.5 and 2 μm gaps. It can be clearly seen that the potential varies almost linearly for both gaps with an almost constant electric field across the gap. For the 0.5 μm gap, the electric field across the entire gap is within 0.002% of the nominal value of 50 V/μm. The PIC/MCC simulations presented above clearly show that the value of α for microscale gaps depends on the actual gap size apart from the electric field. Therefore, microscale gas breakdown models that use macroscale Paschen curve parameters will predict breakdown voltages that are lower than the true breakdown voltages due to their overprediction of α. As a result, a model that describes the correct behavior of α at microscales is formulated using a number of PIC/MCC simulations (detailed tabulated results available in Ref. 28) for various values of electric field and gap size for both argon and nitrogen microdischarges with the results summarized in Figure 4. It should be mentioned that the plot includes data for gap sizes ranging from 0.5 μm to about 8 μm. The E/p values for all these simulations lie between 500 and 1000 V/cm/Torr. The ratio of α/p obtained from PIC/MCC simulations to the value of macroscale α/p obtained using the Paschen parameters is plotted as a function of the voltage normalized

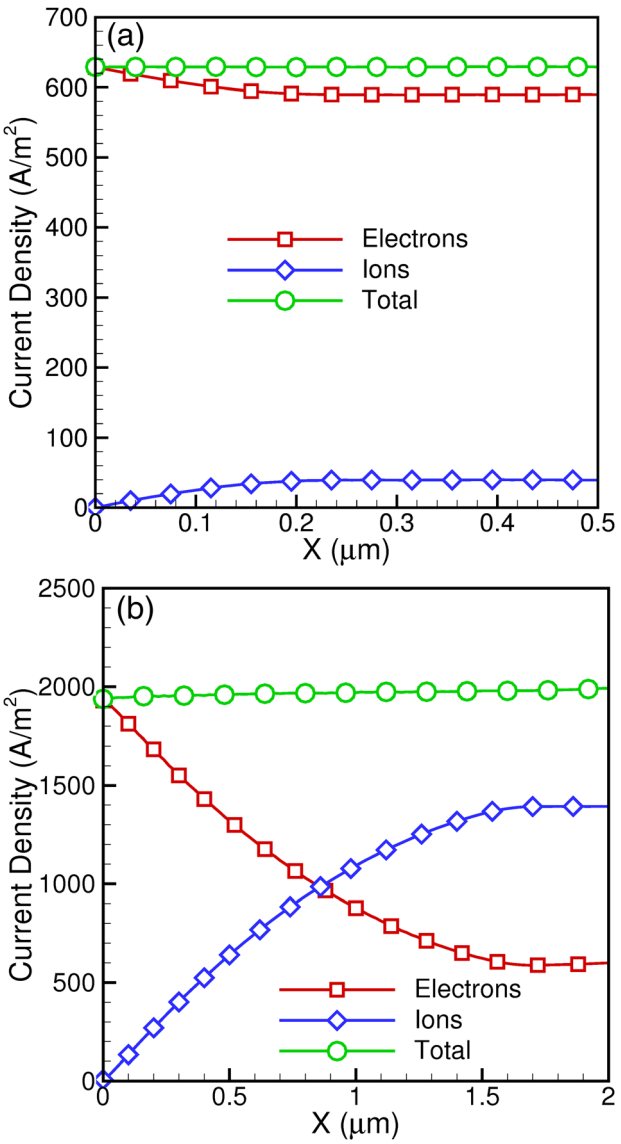

FIG. 2. Comparison of ion and electron current density variation across the gap for 0.5 and 2 μm argon microdischarge at an electric field of 50 V/μm. $j_0 = 616.49\,\mathrm{A/m^2}$ and $\gamma_{se} = 0.0$.

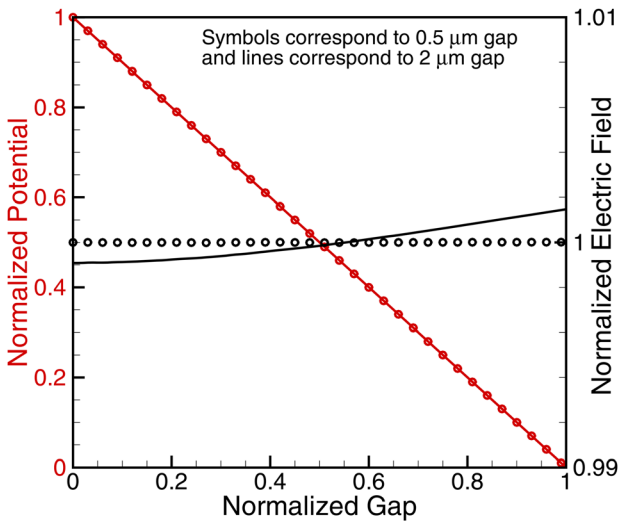

FIG. 3. Comparison of potential and electric field variation across the gap for 0.5 and 2 μm argon microdischarge at an electric field of 50 V/μm. $j_0 = 616.49\,\mathrm{A/m^2}$ and $\gamma_{se} = 0.0$. Symbols correspond to 0.5 μm and lines correspond to 2 μm. Red corresponds to potential and black corresponds to electric field.

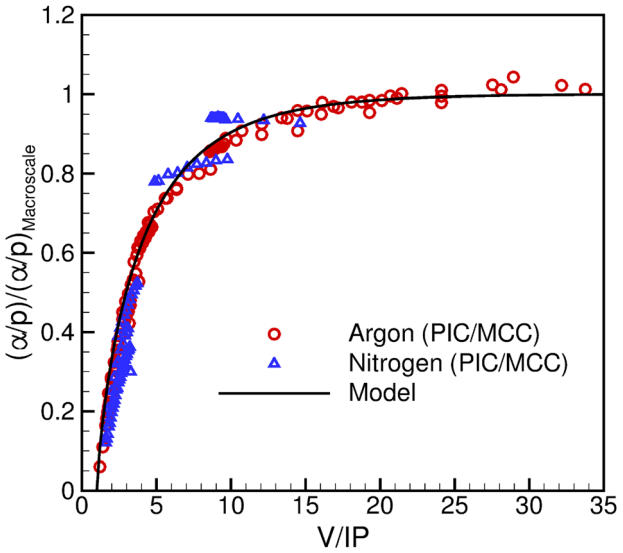

FIG. 4. Comparison of ratio of (α/p) obtained from PIC/MCC simulations to $(\alpha/p)_{\text{Macroscale}}$ for various gap sizes of argon and nitrogen with the proposed ionization coefficient model given by Eq. (9). Gap sizes range from 0.5 to 8 μm with E/p between 500 and 1000 V/cm/Torr for all cases.

with respect to the ionization potential of the gas. It can be seen that when the applied voltage is much higher than the ionization potential, indicating that there are sufficiently large number of ionizing collisions in the gap, the ratio tends to 1 indicating that macroscale models predict the ionization coefficient accurately. However, for voltages comparable to the ionization potential, there is significant deviation from the macroscale α/p with the dependence of deviation on V/IP to be quantified later.

It is also worth discussing the effect of backscattering, which is particularly significant for small values of applied voltage. To explain this effect, let us consider an atmospheric pressure microdischarge with 20 V applied across 0.5 μm. In this microdischarge, an average electron starting from rest at the cathode can participate in a maximum of 1 ionizing collision before it reaches the anode. At these low applied voltages, most of the electron-neutral collisions are elastic due to the significantly higher cross section when compared to other collision mechanisms. Elastic scattering of low-energy electrons are largely isotropic resulting in a reasonable fraction of backscattered electrons, which drift towards the cathode. As a result, for a given cathode source current density j_0, the steady state current density in the gap is less than j_0 corresponding to an effective ionization coefficient that is negative based on Eq. (6). However, it is worth noting that this does not imply the absence of ions in the gap. The increase in current density due to ionization balances the decrease due to backscattering when the applied voltage is about 50% higher than the ionization potential. This essentially corresponds to an effective value of $\alpha = 0$ (based on Eq. (6)) where the cathode source current is not amplified in spite of a few ionizing collisions in the gap. The influence of backscattering could be included in Eqs. (6) and (8) by using a factor but is typically not taken into account since the decrease in current density due to backscattering is only about 5%.

To describe the deviation of the ionization coefficient at applied voltages that are comparable to the ionization potential, we formulate a model that depends on V/IP. This is a parameter that is closely related to the ratio of the ionization mean free path to the gap size ($\lambda/d \sim IP/V$), which in turn determines the number of ionizing collisions. The results from PIC/MCC simulations were observed to be described accurately using a semi-empirical model given by

$$\frac{\alpha}{p} = \left(\frac{\alpha}{p}\right)_{\text{Macroscale}} \left[1 - \exp\left(-\left(\frac{V/IP - 1.0}{3.1}\right)^{0.8}\right)\right], \quad (9)$$

where IP refers to the ionization potential in units of V. The above model is valid for all applied voltages greater than the ionization potential and assumes no ion generation for voltages less than the ionization potential. This assumption is reasonable though not perfectly true due to the fact that the electrons introduced at the cathode location have an energy distribution and there is a small but finite probability for an electron to gain energy higher than the ionization potential even when the applied voltage is less than the ionization potential. For argon, the value of macroscale α/p is given by[6]

$$\left(\frac{\alpha}{p}\right)_{\text{Macroscale}} = C\exp(-D\sqrt{p/E}), \quad (10)$$

where $C = 29.2$ 1/cm/Torr and $D = 26.6$ $\text{V}^{1/2}/\text{cm}^{1/2}/\text{Torr}^{1/2}$, which is considered to lead to better agreements with experiments for inert gases[6] than the model using A_p and B_p. For nitrogen, the values of A_p and B_p were taken from Raizer.[6] The values of Paschen parameters for various common gases are summarized in Table I.

The proposed model was also compared with PIC/MCC simulations for a gap size of 2 μm and various values of pressure. Figure 5 shows the variation of α/p as a function of pressure for a fixed value of $E/p = 1000$ V/cm/Torr. While the value of α/p increases with increasing pressure for pressures in the range 190 Torr to about 1000 Torr, the rate of increase is lower for higher values of pressure with α/p tending to a certain value. The values of α/p at 1500 Torr and 2000 Torr agree within 2%. The model given by Eq. (9) shows good agreement with the PIC/MCC simulations. For example, the α/p value for $p = 380$ Torr, $V = 76$ V, and $d = 2$ μm from actual PIC/MCC simulations is 7.9335 1/Torr/cm, and the model predicts a value of 7.8958

TABLE I. Summary of Paschen parameters from literature for various common gases. Most of the data is from Raizer[6] except for oxygen, which is based on PIC/MCC simulations in this work.

Gas	A_p	B_p	C	D
Helium	3	34	4.4	14
Argon	12	180	29.2	26.6
Nitrogen	12	342		
Oxygen	14	341		
Air	15	365		
Xenon	26	350		

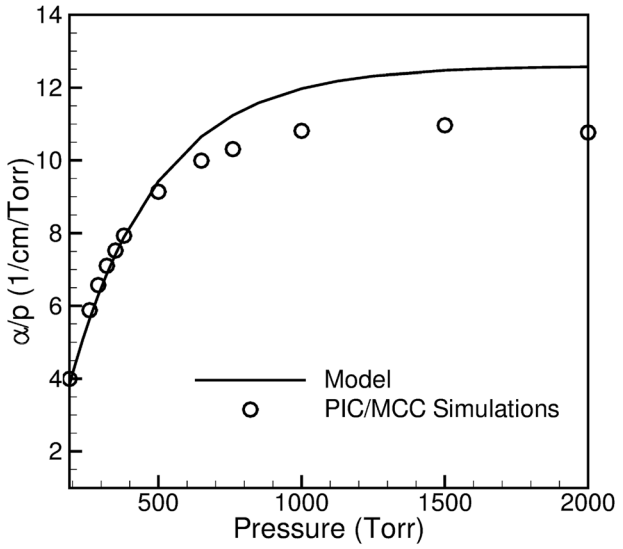

FIG. 5. Variation of α/p as a function of pressure for a given value of $E/p = 1000$ V/cm/Torr obtained from PIC/MCC simulations and the proposed ionization coefficient model given by Eq. (9). The gap size was fixed at 2 μm.

1/Torr/cm, which agrees within 1%. Though the error is higher for a pressure of 2000 Torr, it is still within acceptable limits at 17%.

It should be mentioned that at very high E/p, the value of $\alpha_{\text{Macroscale}}$ obtained using Paschen parameters (for example, Eq. (10)) becomes inaccurate and it would be better to use the most accurate macroscale theory corresponding to such high E/p.[29,30] Strictly speaking, the parameters in Eq. (9) may show a weak dependence on the gas under consideration, but since the ionization cross section variation near the ionization potential is similar for a wide range of gases, the proposed model can be used as a first approximation for the microscale ionization coefficient in the absence of reliable data. However, if data are available at microscales for a certain gas, it is likely to be more accurate than the semi-empirical model proposed here. Since the model proposed in Eq. (9) for deviation from macroscale theories (based on either Paschen parameters or high E/p theories[29,30]) is based on simulations performed for $500 < E/p < 1000$ V/cm/Torr, it is worth evaluating its performance for conditions outside this range of E/p. Here, the performance of the empirical model is demonstrated using PIC/MCC simulations of two argon microdischarges at $E/p = 2000$ V/cm/Torr. The first microdischarge has 456 V applied across 3 μm, and the second microdischarge has 45.6 V applied across 0.3 μm. Since 456 V is much higher than the ionization potential of argon, the value of α/p obtained from this simulation is a good estimate of $(\alpha/p)_{\text{Macroscale}}$, and hence, the ratio of α/p for these two simulations can be used to evaluate the performance of the empirical model at $E/p > 1000$ V/cm/Torr. The ratio of α/p for the two cases was obtained as 0.4904 with Eq. (9), predicting a value of 0.3900 corresponding to an error of about 20%. Therefore, the model describes the deviation from macroscale α/p reasonably well even at E/p values higher than 1000 V/cm/Torr. Here, it should be mentioned that the value of $\alpha_{\text{Macroscale}}$ at these high E/p is better represented by high E/p theories[29,30] since Paschen parameters tend to overpredict[30] the value of α at such high E/p. For example, macroscale α/p at $E/p = 2000$ V/cm/Torr is predicted as 16.1089 1/cm/Torr using Paschen parameters in comparison to 13.2051 1/cm/Torr obtained using PIC/MCC simulations.

B. Ion-enhancement coefficient

The previous section studied ionization in microscale gaps but did not deal with field emission, which is the most important phenomenon for breakdown in microgaps. The role played by the ion-enhancement coefficient γ' is similar to the role played by γ_{se} in macroscale gaps, and its value can be extracted[17] using PIC/MCC numerical experiments. The initial set of simulations were performed for $\beta = 55$, which is a reasonable estimate based on actual microscale structures[16] though the dependence on β will be addressed subsequently. The cathode material was assumed to be nickel with a work function of 5.15 eV. The value of γ_{se} was taken to be 0 without loss of generality. The numerical experiments were performed for gap sizes ranging from 0.5 to 3 μm for the purpose of validation of the model formulated in this work. Figure 6(a) shows the electron and ion current density variation in the gap for an applied voltage of 58 V.

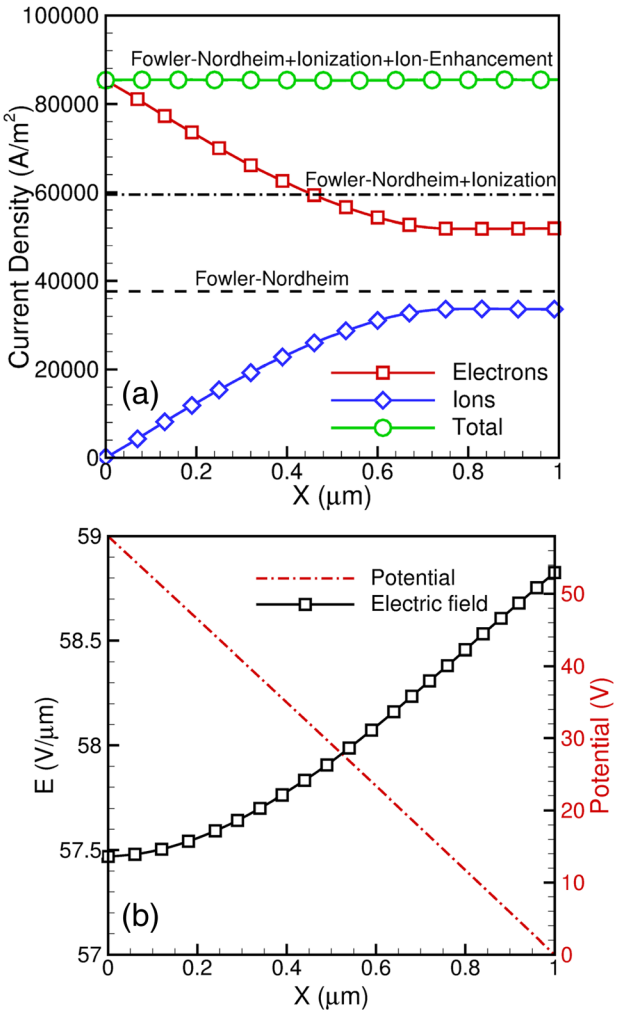

FIG. 6. Current density, potential and electric field variation across the gap for an applied voltage of 58 V across a 1 μm argon gap. The value of $\beta = 55$ and $\gamma_{se} = 0$.

Apart from the total current densities at steady state, the figure also shows the current densities that would correspond to pure F-N emission (using the nominal electric field of 58 V/μm) and F-N emission coupled with ionization in the gas phase. The F-N emission coupled with ionization (labeled as "Fowler-Nordheim+Ionization" was obtained as

$$j_{\mathrm{FN+ion}} = j_{\mathrm{FN}} \exp(\alpha d), \tag{11}$$

where $d = 10^{-4}$ cm, j_{FN} is the F-N current density, and α is obtained using the microscale model presented in Sec. III A. The total PIC/MCC current density at steady state is higher than $j_{\mathrm{FN+ion}}$ by a factor of 1.38. This increase in the total current density is due to the effect of field emission enhancement due to space charge and γ' can be extracted using a relation similar to Eq. (8), where γ_{se} is replaced by γ'. The value of γ' was obtained as 0.4231 for the above case. Even though the electric field at the cathode location, as shown in Figure 6(b) increased by only about 1.43%, it contributes to a significant increase in the F-N current density due to the exponential relation between electric field and F-N current density. Microscale gas breakdown through electron avalanche occurs when the cathode electric field changes by about 3%. A model that describes microscale gas breakdown should have the capability to predict, apart from the total current density, parameters such as γ' and the increase in cathode electric field due to positive space charge in the gap.

In order to formulate such a model, we use an approach similar to that used by Boyle and Kisliuk[7] with suitable modifications as presented below. We can write the F-N equation as

$$j_{\mathrm{FN}} = C_{\mathrm{FN}} E^2 \exp\left(-\frac{D_{\mathrm{FN}}}{E}\right), \tag{12}$$

where E is the applied electric field. The constants C_{FN} and D_{FN} depend on A_{FN}, B_{FN}, β, and ϕ and are given by

$$D_{\mathrm{FN}} = \frac{0.95 B_{FN} \phi^{3/2}}{\beta}, \tag{13}$$

$$C_{\mathrm{FN}} = \frac{A_{\mathrm{FN}} \beta^2}{\phi t^2(y)} \exp\left(\frac{(3.79 \times 10^{-4})^2 B_{\mathrm{FN}}}{\phi^{1/2}}\right). \tag{14}$$

When there is positive space charge in the gap, the cathode electric field is modified to, say, $E + E^+$, where E^+ is the increase in electric field due to the positive space charge. The F-N current density at the enhanced electric field is given by

$$j'_{\mathrm{FN}} = C_{\mathrm{FN}} (E + E^+)^2 \exp\left(-\frac{D_{\mathrm{FN}}}{E + E^+}\right). \tag{15}$$

The change in electric field E^+ is small in comparison to the applied electric field E and the above expression can be simplified, using a Taylor's series expansion on each term involving E^+ and neglecting the higher order terms, to

$$j'_{\mathrm{FN}} = C_{\mathrm{FN}} E^2 \left(1 + \frac{2E^+}{E}\right) \exp\left(\frac{D_{\mathrm{FN}} E^+}{E^2}\right) \exp\left(-\frac{D_{\mathrm{FN}}}{E}\right). \tag{16}$$

This increased F-N current density is enhanced due to ionization in the gap and secondary electron emission, leading to a steady state total current density of

$$\begin{aligned} j_{\mathrm{tot}} &= j'_{\mathrm{FN}} \frac{\exp(\alpha d)}{1 - \gamma_{\mathrm{se}}(\exp(\alpha d) - 1)} \\ &= j_{\mathrm{FN}} \exp\left(\frac{D_{FN} E^+}{E^2}\right) \left(1 + \frac{2E^+}{E}\right) \frac{\exp(\alpha d)}{1 - \gamma_{\mathrm{se}}(\exp(\alpha d) - 1)}. \end{aligned} \tag{17}$$

The total current density can also be written, in terms of γ', as

$$j_{\mathrm{tot}} = \frac{j_{\mathrm{FN}} \exp(\alpha d)}{1 - (\gamma_{\mathrm{se}} + \gamma')(\exp(\alpha d) - 1)}. \tag{18}$$

Comparing the two expressions for j_{tot} gives an expression for γ' as

$$\gamma' = \frac{1 - [1 - \gamma_{\mathrm{se}}(\exp(\alpha d) - 1)] \exp(-D_{\mathrm{FN}} E^+ / E^2)}{(\exp(\alpha d) - 1)(1 + 2E^+/E)} - \gamma_{\mathrm{se}}. \tag{19}$$

It should be mentioned that previous work[7,32] dealing with microscale gas breakdown recommend a variation given by

$$\gamma' = K \exp\left(-\frac{D_{\mathrm{FN}}}{E}\right), \tag{20}$$

where K is a constant. The only unknown parameter in Eq. (17) for total current density and Eq. (19) for γ' is E^+, which is the increase in the cathode electric field due to the positive space charge. Starting from the Poisson's equation, we obtain an approximate expression for the value of E^+. The Poisson's equation is given by

$$\frac{dE}{dx} = \frac{\rho}{\epsilon_0}, \tag{21}$$

where ρ is the charge density and ϵ_0 is the permittivity of free space. Assuming that the electric field at the center of the gap is the nominal electric field (based on results of PIC/MCC simulations) and also a constant charge density from $d/2$ to d, we can write

$$E^+ = \frac{\rho d}{2\epsilon_0}. \tag{22}$$

The charge density can be written in terms of the ion current density (j_{ion}) and the ion drift velocity (v_d) as

$$\rho = \frac{j_{\mathrm{ion}}}{v_d}. \tag{23}$$

The ion current density at the cathode is related to the total current density in the gap through the relation

$$j_{\mathrm{ion}} = \frac{j_{\mathrm{tot}}(\exp(\alpha d) - 1)}{\exp(\alpha d)}. \tag{24}$$

Using Eq. (17), this can be simplified to

$$j_{\text{ion}} = \frac{j_{\text{FN}} \exp\left(\frac{D_{\text{FN}}E^+}{E^2}\right)\left(1+\frac{2E^+}{E}\right)(\exp(\alpha d)-1)}{1-\gamma_{\text{se}}(\exp(\alpha d)-1)}. \quad (25)$$

Therefore, Eq. (22) can be written as

$$E^+ = \frac{dj_{FN}(\exp(\alpha d)-1)}{2v_{\text{d}}\epsilon_0[1-\gamma_{\text{se}}(\exp(\alpha d)-1)]}\exp\left(\frac{D_{\text{FN}}E^+}{E^2}\right)\left(1+\frac{2E^+}{E}\right). \quad (26)$$

Multiplying both sides of the above equation by D_{FN}/E^2 and referring to $D_{\text{FN}}E^+/E^2$ as x, we get an equation of the form

$$\frac{\exp(x)(1+2E^*x)}{F_{\text{br}}x} = 1, \quad (27)$$

where $E^* = E/D_{\text{FN}}$ and F_{br} is a breakdown parameter given by

$$F_{\text{br}} = \frac{2v_{\text{d}}\epsilon_0 E^2[1-\gamma_{\text{se}}(\exp(\alpha d)-1)]}{D_{\text{FN}}dj_{FN}(\exp(\alpha d)-1)}. \quad (28)$$

Solving for this x numerically using, say, Newton's method gives the enhancement in the electric field E^+, which when used in Eqs. (17) and (19) give the values of total current density and γ', respectively. Note that the ion drift velocity is obtained using the expression[33]

$$v_d = \sqrt{\frac{2ekT_gE}{\pi mp\sigma_{\text{CE}}}}, \quad (29)$$

where k is the Boltzmann's constant, T_g is the neutral gas temperature, and σ_{CE} is the charge exchange cross section. The charge exchange cross section typically depends on the energy and the drift velocity obtained should be consistent with the ion energy at which σ_{CE} is computed. The approximate theory formulated above is compared with results from PIC/MCC simulations for various gap sizes ranging from 0.5 to 3 μm at various values of applied voltage with the results summarized in Figure 7, which shows the variation of the total current density at steady state. The results have been plotted as a function of E/p though all cases were simulated at a pressure of 760 Torr. The value of γ_{se} was taken to be 0. The proposed model shows very good overall agreement with the PIC/MCC simulations. It also clearly shows the change in the slope of the current density variation when the applied voltage reaches the breakdown voltage. This was also observed in measurements reported by Hourdakis *et al.*[34] The minor differences between the proposed model and PIC/MCC simulations occur right at breakdown where the simulations consistently predict earlier breakdown by about 0.5–1 V. This discrepancy could be due to some of the simplifying assumptions made while formulating the increase in electric field E^+ at the cathode.

The proposed model was also compared with PIC/MCC simulations performed at a fixed value of βV for 1 and 2 μm gaps. The value of βV was chosen as 3190 V for the 1 μm gap and 5830 V for the 2 μm gap. Fixing the value of βV fixes the value of the nominal field emission current density

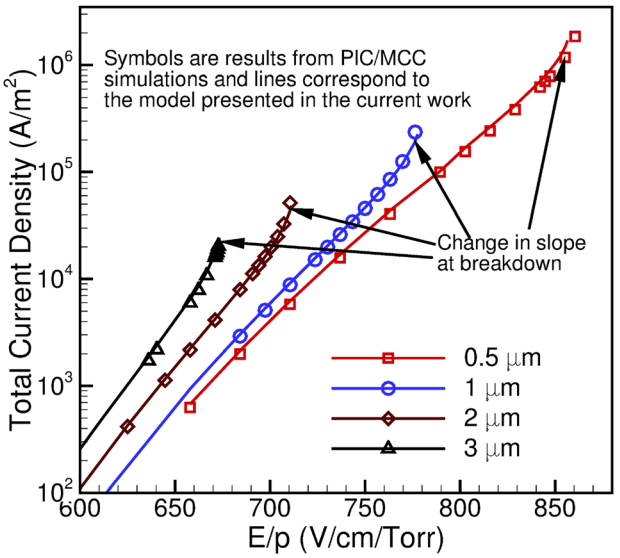

FIG. 7. Comparison of total current density in the gap as a function of E/p for various gap sizes.

(j_{FN}), but the enhancement due to positive space charge will be different depending on the value of β. Also, due to the different applied voltages, the ionization characteristics in the gap are different for the different cases. The PIC/MCC simulations show that the total current density, as shown in Figure 8, decreases with increasing β, indicating that for the lower values of β, the decrease in the ion-enhancement coefficient is compensated by a significantly higher ionization coefficient in the gap. The differences between the simulations and the proposed model at lower values of β can be attributed to the error in computing the ionization coefficient at very high E/p values. For example, the 2 μm case at $\beta = 25$ corresponds to $E/p = 1500$. Since the purpose of this work is not to study high E/p effects, we did not use high E/p ionization coefficient models here. Using the less accurate

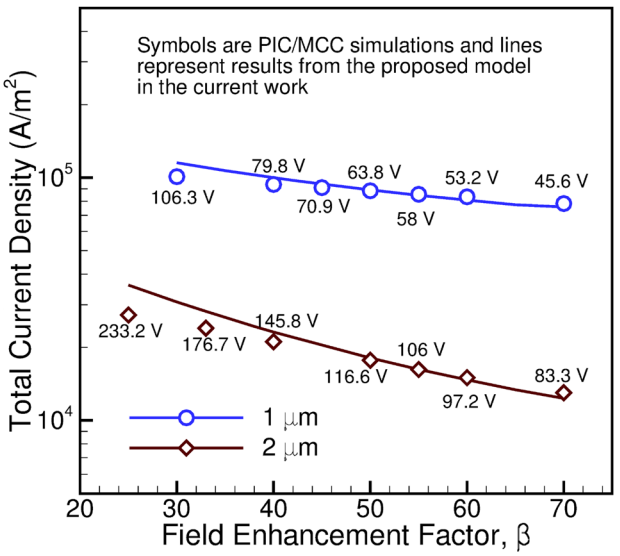

FIG. 8. Comparison of total current density in the gap as a function of β for a fixed value of βV. The value of $\beta V = 3190$ V for 1 μm and $\beta V = 5830$ V for 2 μm.

moderate E/p model at high E/p results in an error of about 20% in α.

C. Avalanche breakdown voltage

In this subsection, the theoretical and semi-empirical models formulated in the previous two subsections are used to predict the breakdown voltage and compare it with the breakdown voltages predicted by PIC/MCC simulations by obtaining the voltage at which the number of electrons and ions in the simulation diverges. The breakdown criteria for the scaling law presented here can be obtained by considering the equation for the enhancement in the cathode electric field, E^+. The value of E^+ is obtained by solving an equation of the form $g(x) = \exp(x)(1 + 2E^*x)/F_{\mathrm{br}}x = 1$. This equation has a solution only when a pre-breakdown steady state exists for the microdischarge under consideration. Specifically, the minimum value of the function $g(x) = \exp(x)(1 + 2E^*x)/F_{\mathrm{br}}x$ can be shown to occur when $x = (\sqrt{1 + 8E^*} - 1)/4E^*$ and no solution exists if $g((\sqrt{1 + 8E^*} - 1)/4E^*) > 1$. In other words, breakdown occurs when $g(\sqrt{1 + 8E^*} - 1)/4E^*) = 1$ is satisfied. Therefore, our breakdown criterion is

$$F_{\mathrm{br}} = \frac{2v_{\mathrm{d}}\epsilon_0 E^2[1 - \gamma_{\mathrm{se}}(\exp(\alpha d) - 1)]}{D_{\mathrm{FN}} d j_{FN}(\exp(\alpha d) - 1)} = \frac{\exp(x_0)(1 + 2E^* x_0)}{x_0}, \tag{30}$$

where $x_0 = (\sqrt{1 + 8E^*} - 1)/4E^*$ lies between 0 and 1 with the value of x_0 tending to 1 for $E^* \ll 1$. Therefore, the right hand side of Eq. (30) has a finite value. At first glance it might seem like this breakdown condition does not retrieve the classical Townsend avalanche criterion in the absence of field emission. However, in the absence of field emission or when field emission effects are extremely small, the denominator goes to 0, which implies the numerator has to approach zero for the ratio to have a finite value. The numerator going to zero directly corresponds to the classical Townsend avalanche criterion of

$$\gamma_{\mathrm{se}}(\exp(\alpha d) - 1) = 1. \tag{31}$$

Figure 9 shows the variation of breakdown voltage as a function of gap size for argon at atmospheric pressure for various values of γ_{se}. When $\gamma_{\mathrm{se}} = 0$, the Paschen curve predicts infinite breakdown voltage. However, if field emission is included, the breakdown voltages are finite as can be seen in Figure 9. With an increase in the value of γ_{se} to 0.01, the classical Paschen curve predicts a finite breakdown voltage. However, for very small gap sizes, the breakdown process is completely determined by the space charge enhancement. For larger gap sizes, the breakdown voltage follows the traditional Paschen curve corresponding to $\gamma_{\mathrm{se}} = 0.01$ since $\gamma' \ll 0.01$ for these gaps. The modified Paschen curve merges with the Paschen curve at about 7 μm for $\gamma_{\mathrm{se}} = 0.01$. With further increase in the value of γ_{se}, the modified Paschen curve merges with the Paschen curve at a gap size of about 3 μm. The proposed breakdown model predicts breakdown voltages that agree extremely well with PIC/MCC simulations. It should be mentioned that obtaining breakdown voltage from PIC/MCC simulations requires several runs at various voltages to observe when the number of ions and electrons in the simulation diverge. Therefore, the PIC/MCC breakdown voltages were obtained only for $\gamma_{\mathrm{se}} = 0$.

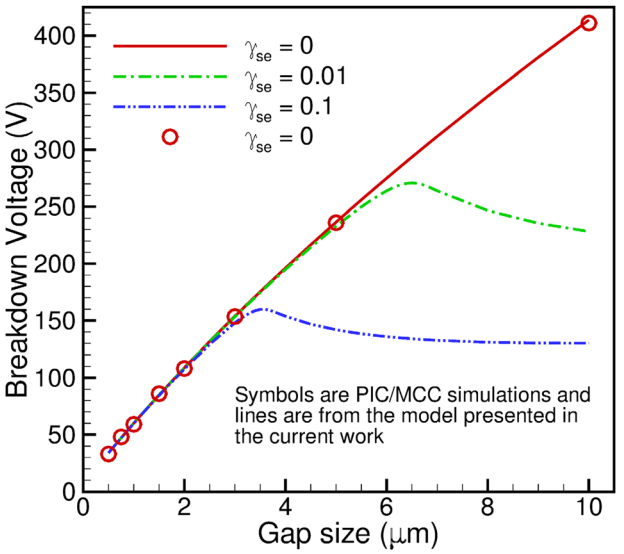

FIG. 9. Comparison of variation of breakdown voltage as a function of gap size for argon obtained from PIC/MCC simulations and the proposed breakdown model.

D. Comparison with experiments

The proposed scaling law for gas breakdown was then used to compare with published experimental data for breakdown in air. The comparisons were performed for two independent sets of experimental data for atmospheric pressure air. The first set by Lee *et al.*[35] (data obtained from Ref. 36) was performed for a polished iron needle cathode, and the

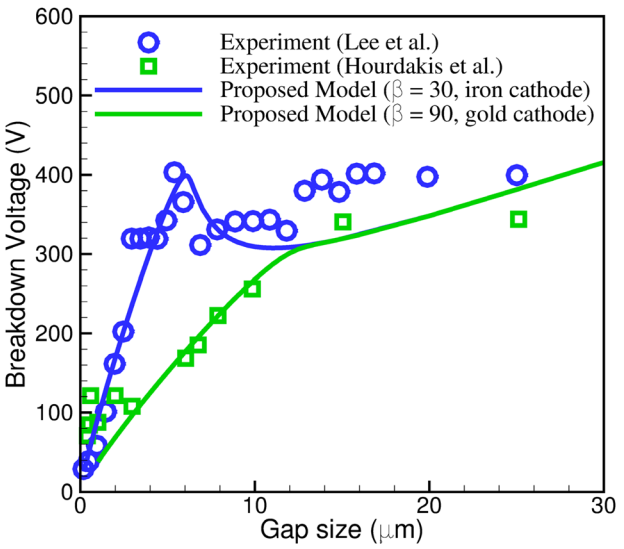

FIG. 10. Comparison of breakdown voltage of atmospheric pressure air obtained using the proposed model and experimental data using iron ($\phi = 4.5$ eV) and gold ($\phi = 5.1$ eV) cathodes. The value of $\gamma_{\mathrm{se}} = 0.01$. The experimental data were obtained from the setup of Hourdakis *et al.*[34] and Lee *et al.*[35] (data extracted from Slade and Taylor[36]).

second set by Hourdakis *et al.*[34] was for a planar gold cathode. The work function of iron and gold were used as 4.5 and 5.1 eV, respectively. The ionization potential for air was used as 14.9 eV, and the Paschen parameters were taken from Raizer.[6] Figure 10 compares results obtained using the proposed breakdown model and the experimental data. It can be seen that the experimental data of Lee *et al.* are described well using a reasonable value of $\beta = 40$ and the experimental data of Hourdakis *et al.* are described using $\beta = 90$. The value of γ_{se} was fixed at 0.01 for both cases and was not fitted to agree better with the experimental data at larger gaps since the main goal was to demonstrate that the models show good agreement for microscale breakdown voltages. Though the value of β is an uncertain parameter as was mentioned earlier, the proposed breakdown model explains the general trend of the experimental data very well. The value of β strongly depends on the method used to fabricate the microscale structure and once a reasonable value of β can be estimated for a particular fabrication technique, the proposed breakdown model can be used to compute the voltage limit beyond which gas breakdown could contribute to the failure of the microscale device.

IV. CONCLUSIONS

The gas breakdown at microscale has been studied using fundamental one-dimensional PIC/MCC numerical experiments and compared with a scaling law proposed in this work. Initially, microscale gaps of argon gas at atmospheric pressure were considered for various gap sizes and the microdischarge structures were compared and contrasted with each other. PIC/MCC simulations of argon and nitrogen microdischarges were used to obtain a general model for the microscale ionization coefficient. An approximate theoretical analysis was used to quantify the space charge enhancement coefficient and its influence on microscale gas breakdown. Closed form analytical expressions were obtained for the increase in cathode electric field, total steady state current density, and the ion-enhancement coefficient. The proposed model was validated using PIC/MCC simulations for gap sizes ranging from 0.5 to 3 μm. The proposed breakdown model was also shown to agree very well with experimental data reported earlier. Being a general breakdown model makes it suitable for use in the design and analysis of microscale electrostatic devices with a direct current voltage bias applied across them. Though the model presented here is for direct current breakdown, it can be extended to cases in which the applied voltage is varying as a function of time.

ACKNOWLEDGMENT

This work was supported by National Science Foundation (NSF) award ECCS-1202095.

[1]R. Gomer, *Field Emission and Field Ionization* (American Institute of Physics, 1992).
[2]Y. Feng and J. P. Verboncoeur, "A model for effective field enhancement for Fowler–Nordheim field emission," Phys. Plasmas **12**, 103301 (2005).
[3]Y. Feng and J. P. Verboncoeur, "Transition from Fowler-Nordheim field emission to space charge limited current density," Phys. Plasmas **13**, 073105 (2006).
[4]Y. Feng, J. P. Verboncoeur, and M. C. Lin, "Solution for space charge limited field emission current densities with injection velocity and geometric effects corrections," Phys. Plasmas **15**, 043301 (2008).
[5]J. M. Meek and J. D. Craggs, *Electrical Breakdown of Gases* (John Wiley & Sons, 1953).
[6]Y. P. Raizer, *Gas Discharge Physics* (Springer, Berlin, 1991).
[7]W. S. Boyle and P. Kisliuk, "Departure from Paschen's law of breakdown in gases," Phys. Rev. **97**(2), 255 (1955).
[8]L. H. Germer, "Electrical Breakdown between Close Electrodes in Air," J. Appl. Phys. **30**(1), 46–51 (1959).
[9]P. Kisliuk, "Electron emission at high fields due to positive ions," J. Appl. Phys. **30**(1), 51–55 (1959).
[10]J. M. Torres and R. S. Dhariwal, "Electric field breakdown at micrometre separations," Nanotechnology **10**, 102–107 (1999).
[11]D. B. Go and D. A. Pohlman, "A mathematical model of the modified Paschen's curve for breakdown in microscale gaps," J. Appl. Phys. **107**(10), 103303–103303 (2010).
[12]A. J. Wallash and L. Levit, "Electrical breakdown and ESD phenomena for devices with nanometer-to-micron gaps," Proc. SPIE **4980**, 87–96 (2003).
[13]M. Radmilovic-Radjenovic and B. Radjenovic, "The influence of ion-enhanced field emission on the high-frequency breakdown in microgaps," Plasma Sources Sci. Technol. **16**, 337–340 (2007).
[14]M. Radmilovic-Radjenovic, J. K. Lee, F. Iza, and G. Y. Park, "Particle-in-cell simulation of gas breakdown in microgaps," J. Phys. D: Appl. Phys. **38**, 950 (2005).
[15]M. Radmilovic-Radjenovic and B. Radjenovic, "A particle-in-cell simulation of the high-field effect in devices with micrometer gaps," IEEE Trans. Plasma Sci. **35**, 1223–1228 (2007).
[16]A. Garg, A. Venkattraman, A. Kovacs, A. Alexeenko, and D. Peroulis, "Direct measurement of field emission current in E-Static MEMS structures," in 24th International Conference on Micro Electro Mechanical Systems, 412–415 (2011).
[17]A. Venkattraman, A. Garg, D. Peroulis, and A. A. Alexeenko, "Direct measurements and numerical simulations of gas charging in microelectromechanical system capacitive switches," Appl. Phys. Lett. **100**(8), 083503–083503 (2012).
[18]R. Tirumala and D. B. Go, "An analytical formulation for the modified Paschen's curve," Appl. Phys. Lett. **97**, 151502 (2010).
[19]W. Zhang, T. S. Fisher, and S. V. Garimella, "Simulation of ion generation and breakdown in atmospheric air," J. Appl. Phys. **96**, 6066 (2004).
[20]R. H. Fowler and L. W. Nordheim, "Electron emission in intense electric fields," Proc. R. Soc. London, Ser. A **119**(781), 173–181 (1928).
[21]R. E. Burgess, H. Kroemer, and J. M. Houston, "Corrected values of Fowler-Nordheim field emission functions v (y) and s (y)," Phys. Rev. **90**, 515 (1953).
[22]T. E. Stern, B. S. Gossling, and R. H. Fowler, "Further studies in the emission of electrons from cold metals," Proc. R. Soc. London, Ser. A. **124**(795), 699–723 (1929).
[23]C. K. Birdsall, Particle-in-Cell Charged-Particle Simulations, Plus Monte Carlo Collisions With Neutral Atoms, PIC-MCC, IEEE Trans. Plasma Sci. **19**(2), 65–85 (1991).
[24]C. K. Birdsall and A. B. Langdon, *Plasma Physics Via Computer Simulation* (Taylor and Francis, 2004).
[25]J. P. Verboncoeur, "Particle simulation of plasmas: review and advances," Plasma Phys. Contr. F. **47**, A231 (2005).
[26]J. P. Verboncoeur, M. V. Alves, V. Vahedi, and C. K. Birdsall, "Simultaneous potential and circuit solution for 1 D bounded plasma particle simulation codes," J. Comput. Phys. **104**, 321–328 (1993).
[27]J. A. Bittencourt, *Fundamentals of Plasma Physics* (Springer-Verlag, 2004).
[28]A. Venkattraman, "Particle simulations of ion generation and transport in microelectromechanical systems and microthrusters," Ph.D. dissertation (Purdue University, Indiana, 2012).
[29]L. Friedland, "Electron multiplication in a gas discharge at high values of E/P," J. Phys. D: Appl. Phys. **7**(16), 2246 (1974).
[30]Y. I. Davydov, "On the first Townsend coefficient at high electric field," IEEE Trans. Nucl. Sci. **53**(5), 2931–2935 (2006).
[31]P. Rumbach and D. B. Go, "Fundamental properties of field emission-driven direct current microdischarges," J. Appl. Phys. **112**, 103302 (2012).
[32]M. Radmilovic-Radjenovic and B. Radjenovic, "Theoretical study of the electron field emission phenomena in the generation of a

micrometer scale discharge," Plasma Sources Sci. Technol. **17**, 024005 (2008).
[33]A. V. Phelps and B. M. Jelenkovic, "Excitation and breakdown of Ar at very high ratios of electric field to gas density," Phys. Rev. A **38**, 2975 (1988).
[34]E. Hourdakis, B. J. Simonds, and N. M. Zimmerman, "Submicron gap capacitor for measurement of breakdown voltage in air," Rev. Sci. Instrum. **77**, 034702 (2006).
[35]R. T. Lee, H. H. Chung, and Y. C. Chiou, "Arc erosion behaviour of silver electric contacts in a single arc discharge across a static gap," in IEE Proceedings of Science, Measurement and Technology (IET, 2001), Vol. 148, pp. 8–14.
[36]P. G. Slade and E. D. Taylor, "Electrical breakdown in atmospheric air between closely spaced (0.2 μm–40 μm) electrical contacts," IEEE Trans. Compon. Packaging Technol. **25**(3), 390–396 (2002).